Rheology of Liquid Crystalline Elastomers in Their Isotropic and Smectic A State

J. Weilepp,*,†,‡ J. J. Zanna,‡,§ N. Assfalg,|| P. Stein,‡,|| L. Hilliou,‡ M. Mauzac,⊥ H. Finkelmann,|| H. R. Brand,† and P. Martinoty‡

Theoretische Physik III, Universität Bayreuth, D 95440 Bayreuth, Germany; Centre de Recherche Paul Pascal - C.N.R.S., Domaine Universitaire, Av. du Dr. Schweitzer, F 33600 Pessac, France; Institut für Makromolekulare Chemie, Universität Freiburg, D 79104 Freiburg, Germany; Laboratoire de Dynamique des Fluides Complexes, Unité Mixte de Recherche U.L.P.-C.N.R.S. n°7506, 4 rue Blaise Pascal, F 67070 Strasbourg Cedex, France; and Laboratoire des Interactions Moleculaires et de Réactivité Chimique et Photochimique, Unité Mixte de Recherche U.P.S.-C.N.R.S. n°5623, 118 route de Narbonne, F 31062 Toulouse Cedex, France

Received January 20, 1999; Revised Manuscript Received April 12, 1999

ABSTRACT: The dynamics of two different side-chain liquid crystalline elastomers (SCLCE) exhibiting a smectic A phase is investigated by low-frequency shear and compression experiments. We find that both the isotropic and the smectic A phase have their own characteristic viscoelastic behavior, which seems to be independent of the compound under investigation and thus universal. The relaxation in the isotropic phase shows a distribution of relaxation times, which gives rise to a scaling law of the elastic moduli with an exponent of 0.5. The viscoelastic response in the smectic A phase, however, exhibits a much broader spectrum of relaxation times containing very long-lived modes. It appears that there exists a low-frequency scaling law with an exponent of 0.3 characterizing the smectic A phase. We propose that this result stems from a transient smectic network with a very long lifetime that was set up by the smectic domains. At the phase transition, this transient smectic network disappears, which leads to a sharp decrease of the dynamic shear as well as the compression modulus.

1. Introduction and Motivation

Side-Chain Liquid Crystalline Polymers (SCLCP), i.e., polymeric systems for which mesogenic moieties are attached to the backbone via a flexible chain called a spacer, have been subject to mechanical experiments since they were first synthesized in 1978.[1] Because of their viscoelastic behavior or, more physically, their transient network, they open a wider range of possibilities to couple dynamically to their liquid crystalline order by mechanical fields than do low-molecular-weight liquid crystals. The emerging physical consequences and their influence on the critical behavior close to phase transitions have been studied intensely experimentally[2−7] as well as theoretically.[8−13] In the strictly static limit, however, they behave as their low-molecular-weight counterparts.[14]

This situation changes drastically when the polymer is chemically cross-linked and thus forms a three-dimensional permanent network.[15] These so-called Side-Chain Liquid Crystalline Elastomers (SCLCE) preserve their mesomorphic properties, if the cross-linking density is low enough ($\lesssim$15%).[16,17] In such systems, a static mechanical stress couples directly to the liquid crystalline order[8,18,19] and can therefore be used to induce a reversible polydomain−monodomain transition. This effect is now commonly used for the synthesis of macroscopically ordered monodomains of SCLCEs, the so-called "Liquid Single Crystal Elastomers" (LSCE).[20−23] In these monodomain systems, a stress-induced liquid crystalline order is chemically frozen (cf. Küpfer and Finkelmann[20] and Brand and Kawasaki[24]) by a further cross-linking step. From a dynamical point of view, the permanent network in SCLCEs hinders a macroscopic flow. Consequently, rheological experiments in these systems open the possibility to study directly the influence of the liquid crystalline side-chains on the local flow properties. After the first viscoelastic experiments done on SCLCEs were reported by Oppermann et al. in 1982,[25] work on this interesting topic was recently resumed by Gallani et al.[26,27] In their experiments;[26,27] the emphasis is laid on the rheological properties of a polydomain sample close to the isotropic−nematic and the nematic−smectic A transitions. It is pointed out there that the rheological behavior of the SCLCEs does not change when crossing an isotropic−nematic transition, whereas there is a crucial change at the nematic−smectic A transition. Interestingly, this observation has also been reported for SCLCPs.[7] Very recently, rheological measurements on smectic A monodomains of side-chain[28] as well as main-chain elastomers[29] have been started. These experiments are the dynamic continuation of the static experiments performed on smectic A (side-chain) LSCEs[21] to investigate their striking anisotropic elastic properties.

In this paper, we investigate the rheological properties of two different SCLCE compounds exhibiting an isotropic−smectic A transition by dynamical shear experiments. We find that within each phase they behave qualitatively similar, even though the compounds under investigation as well as the molar fraction of mesogenic side-groups vary drastically. By comparing our results with published data for SCLCPs in their smectic phase,[5−7] we find that the universal behavior observed in the smectic A phase is even found in polymeric systems with totally different chemical structures.

We present two possible interpretations for the relaxation processes in the isotropic as well as the nematic phase (for the latter, the experimental results have been

† Universität Bayreuth.
‡ Laboratoire de Dynamique des Fluides Complexes.
§ Centre de Recherche Paul Pascal.
|| Universität Freiburg.
⊥ Laboratoire des Interactions Moleculaires et de Réactivité Chimique et Photochimique.

10.1021/ma9900838 CCC: $18.00
Published on Web 06/16/1999

presented in Gallani et al.[26]). For the behavior in the smectic A phase, we give a qualitative picture that interprets the dominant effect as the consequence of a complex network set up by the smectic domains, which crucially slows the dynamics of the system.

Finally, we present dynamic compression experiments performed on one of the two compounds used for the shear experiments and show that the materials behave similarly under shear and compression.

2. Background

One of the most crucial differences between the dynamics in viscoelastic fluids such as polymer melts and simple fluids such as water is the spectrum of relaxation times.[30] While in the latter case most processes take place on microscopic time and length scales, such a clear-cut scale separation and therefore a macroscopic dynamic description of viscoelastic systems is rather subtle.

The low wavenumber (k) and low-frequency (ω) behavior of a simple fluid can be modeled by the use of conservation laws, such as mass and momentum conservation. This description requires that all processes taking place on microscopic time (τ_m) and length (λ_m) scales have already decayed, i.e., $\omega\tau_m \ll 1$ and $k\lambda_m \ll 1$, and therefore, the system is in local thermodynamic equilibrium (for further details, see Forster[30]). The regime where this description is valid is called the hydrodynamic regime. The hydrodynamic description of a condensed system becomes exact in the limit $\omega \rightarrow 0$ and $k \rightarrow 0$.

In a viscoelastic liquid, the situation is more complicated. Because of steric hindrance, topological entanglements, and so on, the polymer relaxation is crucially slowed to mesoscopic or even macroscopic scales, so that excitations with a frequency on the order of 1 Hz (as will be shown below) could already be nonhydrodynamic. In a simple fluid, however, even frequencies on the order of 1 MHz lead to a purely hydrodynamic response. Increasing the frequency in the nonhydrodynamic regime gradually leads to an increasing number of frozen degrees of freedom, i.e., internal modes that cannot relax within the typical time scale given by the excitation signal. Above a certain frequency, all degrees of freedom are frozen, and the system is in the dynamic glassy state and thus far away from thermodynamic equilibrium. The entire nonhydrodynamic regime for frequencies below those characterizing the dynamic glassy state is called the dynamic glass transition.

Whereas an elastic solid in its hydrodynamic regime responds with the phase shift $\varphi \equiv 0$ (for a viscous liquid this phase shift is $\varphi = \pi/2$) to a shear excitation if dissipation is neglected, a viscoelastic solid as well as a viscoelastic fluid show a memory with respect to earlier times and therefore respond with a phase shift $0 < \varphi < \pi/2$. In the glassy state, the response is again instantaneous, i.e., $\varphi \equiv 0$, but now, this reflects that no single mode in the system is able to relax within the characteristic excitation time.

In the experiment, which will be described in the following, we investigate the linear response of a viscoelastic material, namely, a side-chain liquid crystalline elastomer, exposed to spatially homogeneous dynamic shear and compression deformations.

Small elastic deformations of a solid are commonly described with the symmetric gradient of the displacement field $\boldsymbol{u}(\boldsymbol{r})$, the strain tensor $\epsilon_{ij} = {}^1/_2(\partial_i u_j + \partial_i u_i)$. A sufficiently small homogeneous deformation applied to the solid usually leads to a linear relation between the applied deformation ϵ and the resulting stress (tensor) $\boldsymbol{\sigma}$, the so-called Hooke's law. In its most general formulation, this linear stress−strain relation reads for an isotropic solid[31]

$$\sigma_{ij} = K\epsilon_{kk}\delta_{ij} + 2G'_{st}(\epsilon_{ij} - {}^1/_3\delta_{ij}\epsilon_{kk}) \qquad (1)$$

where summation over repeated indices is implied. The first contribution models volume dilatational deformations, and therefore, the corresponding elastic modulus K is called the volume compression modulus. The second contribution is trace-free and describes purely volume conserving processes as, for example, shear deformations. Consequently, the elastic modulus G'_{st} is the (static) shear modulus. Experiments in which a homogeneous stress (compression) σ_{zz} is imposed on the elastic solid in the z-direction and the boundaries are stress-free probe the compression modulus of the solid

$$E'_{st} = \frac{\sigma_{zz}}{\epsilon_{zz}} = \frac{9K\,G'_{st}}{3K + G'_{st}} \qquad (2)$$

which is called Young's modulus in the case of static deformations. For incompressible materials, that is $K \rightarrow \infty$, this equation simplifies to $E'_{st} \rightarrow 3G'_{st}$.

In the following, we concentrate on externally applied spatially homogeneous dynamic excitations, that is shear and compression deformations. If one neglects dissipation, which is a good approximation for small-amplitude deformations, one simply probes the dynamic generalization of Hooke's law, and therefore, the measured moduli $G' = \sigma_{xz}/\epsilon_{xz}$ and $E' = \sigma_{zz}/\epsilon_{zz}$ essentially recover the static values. We note that for higher frequencies, i.e., in the nonhydrodynamic or viscoelastic regime, these static values appear as a constant background.

3. Experimental Section

Compounds. For our studies, we use two different kinds of side-chain liquid crystalline elastomers. Both consist of the same polymeric backbone but completely different mesogens. Moreover, the molar fraction of the mesogens varies drastically, but nevertheless, both compounds exhibit a smectic A phase. Whereas sample A might exhibit a very narrow nematic regime,[32] which cannot be observed directly, for example, by differential scanning calorimetry (DSC) (cf. discussion of sample A), sample B shows an isotropic-to-smectic A transition. For the rheological experiments presented below, this qualitative difference in the mesomorphism of the two samples is of minor importance, because one can hardly distinguish an isotropic and a nematic phase of a SCLCE by rheological experiments, as has been reported in Gallani et al.[26] (below, we will give a qualitative explanation for this observation). Therefore, we will refer to the phase-transition region as T_{I-A}, if we address the phenomena being observed for both samples to simplify the notation in the Experimental and the Discussion section of this paper.

Sample A. The compounds used in the synthesis of sample A are presented in Figure 1a. The composition of this liquid crystalline elastomer is 90 mol % (related to the reactive Si−H groups) of the mesogens (40 mol % of R_1 and 50 mol % of R_2) and 10 mol % of the bifunctional hydrochinone derivative (R_3) as cross-

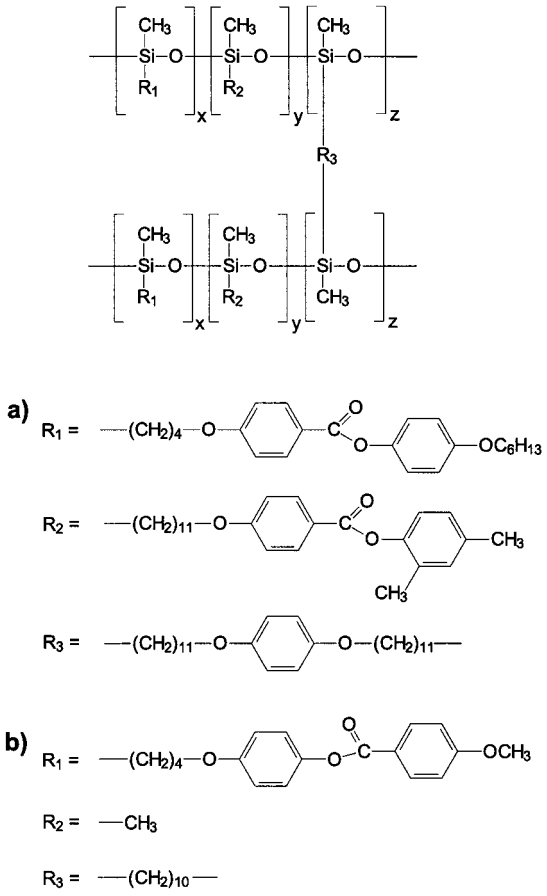

Figure 1. Polydomain SCLCEs based on a polysiloxane backbone. Both compounds exhibit a polydomain smectic A phase. (a) Sample A consists of two kinds of mesogens with a spacer length of 4 (R_1) or 11 (R_2) methylene groups and the crosslinking agent (R_3). The corresponding concentrations are x:y:z = 0.4:0.5:0.1. Phase transitions: glass −18 °C smectic A 62 °C isotropic. (b) Sample B has only one mesogenic unit with a spacer length of 4 (R_1) methylene groups, a methyl group (R_2), and a short aliphatic crosslinker (R_3) with the concentration ratio x:y:z = 0.25:0.70:0.05. Phase transitions: glass −28 °C smectic A 9 °C isotropic.

linker, i.e., x:y:z = 0.4:0.5:0.1. The synthesis of these different compounds is described in Finkelmann and Rehage.[33] The mesogenic compounds (R_1 and R_2), the cross-linker (R_3), and poly(hydrogenmethylsiloxane) as polymer backbone were concurrently dissolved in toluene. The SCLCE is prepared by a platinum-catalyzed hydrosilylation reaction during spin-casting at 60 °C for 3 h. After cross-linking, the elastomer is deswollen on a water surface and dried under vacuum. The phase behavior of the sample has been examined by X-ray measurements and DSC. DSC measurements were performed on a Perkin-Elmer DSC-7. The elastomer exhibits a smectic A phase (layer spacing d = 29 Å) between the glass-transition temperature $T_G = -18$ °C and +58 °C. Above a temperature of 65 °C, the elastomer is in its isotropic state. As discussed above, the mesomorphism of the polydomain sample in the transition region 58 °C $\lesssim T \lesssim$ 65 °C is difficult to determine.

Sample B. Sample B (Figure 1b) is prepared by a one-step hydrosilylation reaction[36] between the hydrogenmethylsiloxane units and the vinyl end-groups of the different substituents. A flat reactor fitted with a reflux condenser is dried with a stream of nitrogen. A mixture of mesogenic groups, cross-linking agents (1−9 decadiene), and copoly(hydrogenmethyl dimethylsiloxane) was

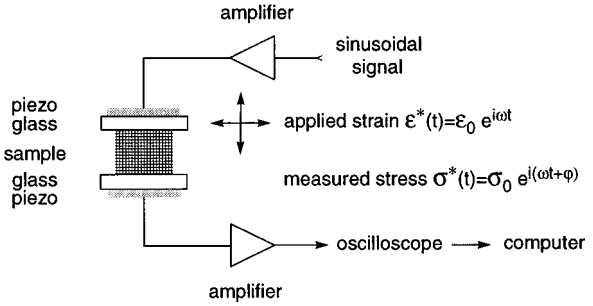

Figure 2. Schematic representation of the piezo-rheometer. Depending on the polarization of the piezo-ceramic elements, the cell can be used to perform dynamic shear (↔) or compression (↕) experiments, respectively.

dissolved at 60 °C in dry toluene. The synthesis of the copolymer is described elsewhere.[37] Vinyl groups exceed hydrogenmethylsiloxane groups by 15%. The reaction is initiated with dicyclopentadienyl platinum(II) (500 ppm with regard to the hydrogenmethylsiloxane groups) and takes place at 60 °C during 1 day. A highly concentrated reaction solution is required to achieve the complete gel formation (2 mmol of siloxane units/mL). After the reaction, the sample is washed in an excess of toluene for 1 week with the solvent being renewed each day. The sample is then deswollen in successive mixtures of toluene and methanol with the methanol fraction being increased in each step.

The elastomer under investigation is composed of 25 mol % mesogenic groups R_1 and 5 mol % cross-linking agent R_3, i.e., x:y:z = 0.25:0.7:0.05. The phase behavior of the LCE is determined by differential scanning calorimetry (Perkin-Elmer DSC 7) showing the glass-transition temperature at $T_G = -28$ °C (heating rate +10 K min^{-1}) and the smectic A to isotropic transition temperature at $T_{I-A} = 9$ °C (cooling rate −5 K min^{-1}). The layer spacing d for sample B at room temperature is d = 46.3 Å.

Experiment. *The Piezo-Rheometer.* For our experiments, we use a piezo-rheometer as schematically shown in Figure 2. The sample is placed between two parallel glass plates; one of them is excited by a piezo-ceramic plate oscillating horizontally or vertically depending on the polarization of the piezo-electric ceramic in use. The applied strain $\epsilon^*(t) = \epsilon_0 \exp(i\omega t)$ is transmitted through the sample, and the second plate detects the resulting stress $\sigma^*(t) = \sigma_0 \exp[i(\omega t + \varphi)]$ via another piezo-ceramic plate polarized in the same direction as the excitation element. Depending on the polarization of the piezo-ceramic elements, either horizontal or vertical, the setup allows measurements of the dynamic shear modulus $G^* = G' + iG''$ or compression modulus $E^* = E' + iE''$, respectively, as complex stress−strain ratio $\sigma^*/\epsilon^* = \sigma_0/\epsilon_0 \exp(i\varphi)$. The piezo-elements in use guarantee very small strain amplitudes of $\epsilon_0 < 10^{-3}$, so that the experiments presented below are all performed in the regime of linear response. The parallelism of the glass plates is controlled by optical interference (Newton's rings) with an accuracy of $\sim 5 \times 10^{-4}$ rad. The cell itself can be operated in the temperature range −30 °C $\leq T \leq$ 160 °C and the frequency range 0.1 Hz $\leq \nu \leq$ 2 kHz.

Experimental Procedure. All experiments presented subsequently are performed using the same experimental procedure. First, the sample is heated to a maximum temperature in the isotropic state. Then, it is cooled step by step to the glass-transition temperature (shear) or

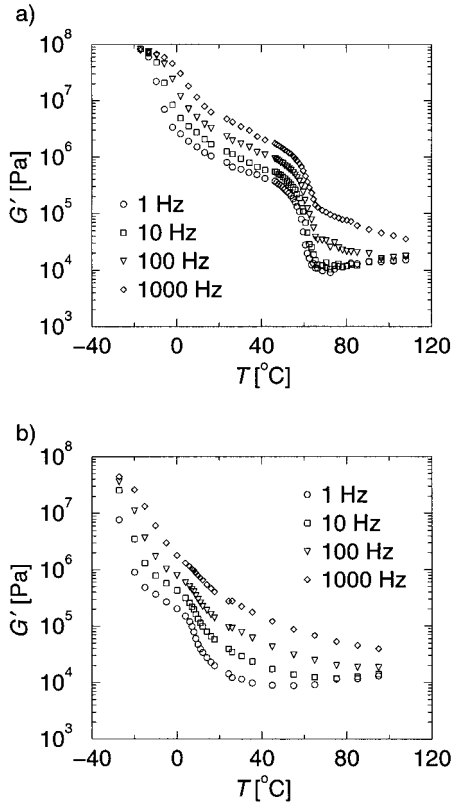

Figure 3. Temperature dependence of the storage modulus $G'(T)$ taken at $\nu = 1$, 10, and 100 Hz and 1 kHz for (a) sample A and (b) sample B.

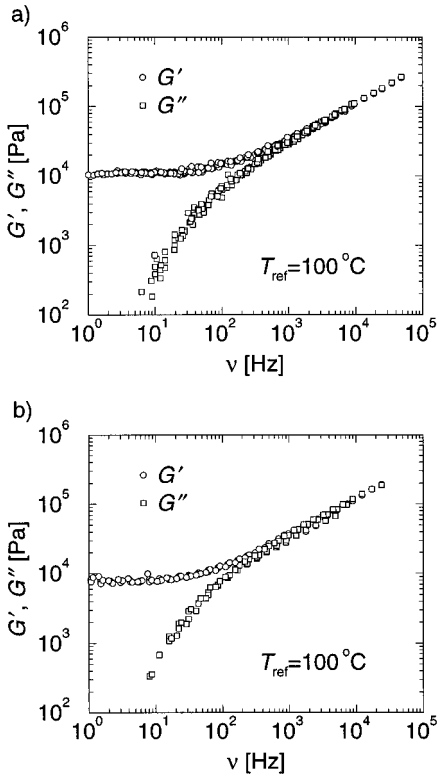

Figure 4. Master curves of G' and G'' in the isotropic phase. (a) Sample A (the curves are obtained from the superposition of measurements taken at 100, 98, 94, 90, 83, 79, 75, and 65 °C) (b) Sample B (the curves are obtained from the superposition of measurements taken at 100, 95, 85, and 75 °C).

well inside the smectic A phase (compression), respectively. After each cooling step, the sample has at least 45 min to equilibrate before the measurements are started. For the experiments done in the isotropic phase, this time is much longer than the longest relaxation time, as will be shown later. In the smectic A phase, the situation will turn out to be different, because there the longest relaxation times can easily exceed days. Nevertheless, we expect the results presented below for the smectic A phase to be at least qualitatively correct.

Results. *Shear Experiments.* The temperature-dependent measurements of the storage modulus $G'(T)$ of samples A and B, respectively, for four different frequencies 1, 10, and 100 Hz and 1 kHz are presented in the Figure 3a,b. The characteristic shape of $G'(T)$ is most pronounced in the 1 Hz curves. They start with a maximum value reflecting the glass-transition temperature with a typical glass modulus $G'_G \approx 10^8$ Pa. Above the glass transition, $G'(T)$ drops first rapidly, later moderately, when approaching the phase-transition temperature T_{I-A} from below. Close to the phase transition, $G'(T)$ decreases more steeply, resulting in a "step", where G' drops by more than 1 order of magnitude within a temperature range of 5−10 K. As the phase-transition temperature of sample B is closer to T_G, the "step" at T_{I-A} is nearly hidden by the dynamic glass transition. A similar result has been reported in Gallani et al.[26] for a smectic A−nematic transition. Because sample A exhibits an extraordinarily broad smectic A regime of 80 K, the transition from the isotropic to the smectic A phase can be observed directly in $G'(T)$ even for very high frequencies. The curves representing the higher frequencies are successively shifted to higher values of $G'(T)$, which is a typical feature of the dynamic glass transition[34,35] with a broad spectrum of relaxation times. In the isotropic phase far above the transition, the curves converge to a frequency-independent curve characterizing an isotropic network being "swollen" by the mesogenic side groups in its hydrodynamic regime.

The master curves of the frequency dependent moduli $G'(\nu)$ and $G''(\nu)$ for the isotropic phase are plotted in Figure 4a,b. They are obtained by using the empirical time−temperature superposition principle[34,35] for the reference temperature $T_{ref} = 100$ °C. Both curves start with a plateau for G' characterizing the permanent network as already discussed in Gallani et al.[26] For higher frequencies, the moduli $G'(\nu)$ and $G''(\nu)$ increase, thus giving rise to a power law behavior $G'(\nu), G''(\nu) \propto \nu^{\zeta}$ characterizing the isotropic phase with the exponents $\zeta^A = 0.50 \pm 0.02$ (sample A) and $\zeta^B = 0.50 \pm 0.05$ (sample B). To increase the accuracy of the superposition and to better elucidate where time−temperature superposition fails, all of the master curves in this paper are obtained by superposition of the phase shift φ between the excitation and the receiving signal. The corresponding master curves $\varphi(\nu)$ are presented in Figure 5a,b. Apart from the observation that the time−temperature superposition principle works very well in the isotropic phase for both samples, a characteristic shape of the $\varphi(\nu)$ curves can be observed: for $\nu \lesssim 10$ Hz, they assume a low-frequency value of $\varphi \approx 0°$, thus indicating that the hydrodynamic regime ($\omega\tau \ll 1$) is very narrow ($\nu \lesssim 10$ Hz) in these elastomeric compounds even far above T_G (more than 100 K). The phase shift $\varphi(\nu)$ increases strongly with frequency and finally arrives at a constant value of $\varphi = (45 \pm 3)°$. To reach higher frequencies on the master curve, measurements at lower temperatures are necessary. Because of the

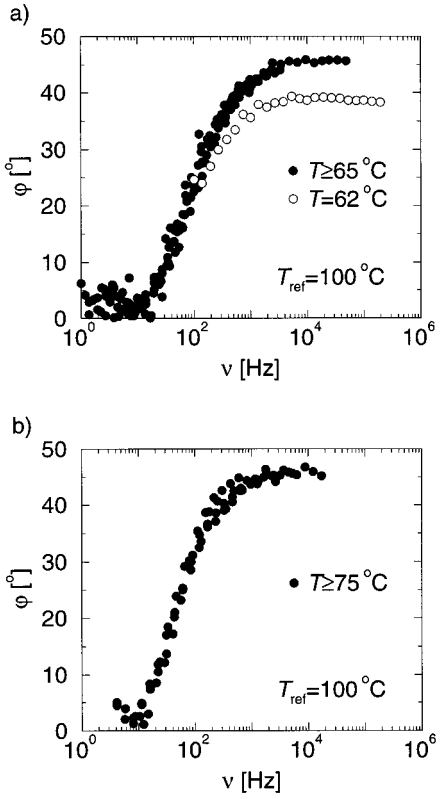

Figure 5. Master curves for the phase shift φ taken at the same temperatures as the master curves in Figure 4. Note the saturation of the curve corresponding to the isotropic phase at the value $\varphi = 45°$ for higher frequencies.

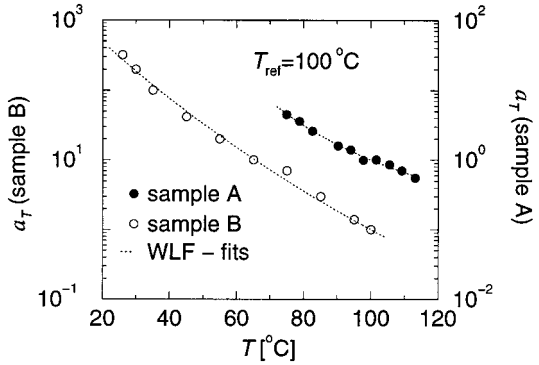

Figure 6. Shift factors a_T used for superposition of the curves in the isotropic phase and corresponding fit with the WLF law.

phase transition to a phase with positional order, this is impossible, as the time−temperature superposition principle fails here. This can be clearly seen in Figure 5a, where we have tried to superimpose $\varphi(\nu)$ for $T = 62$ °C on the master curve.

As can be seen in Figure 6, the shift factors a_T for both samples (but more convincingly for sample B, which has a narrower smectic A phase) can be fitted rather well to the phenomenological Williams−Landel−Ferry law (WLF):[34,35]

$$\log a_T = -C_1 \frac{T - T_{\text{ref}}}{T - T_{\text{ref}} + C_2} \qquad (3)$$

with the fit parameters

$$C_1 = \log e \frac{T_A}{T_{\text{ref}} - T_V} \quad \text{and } C_2 = T_{\text{ref}} - T_V \qquad (4)$$

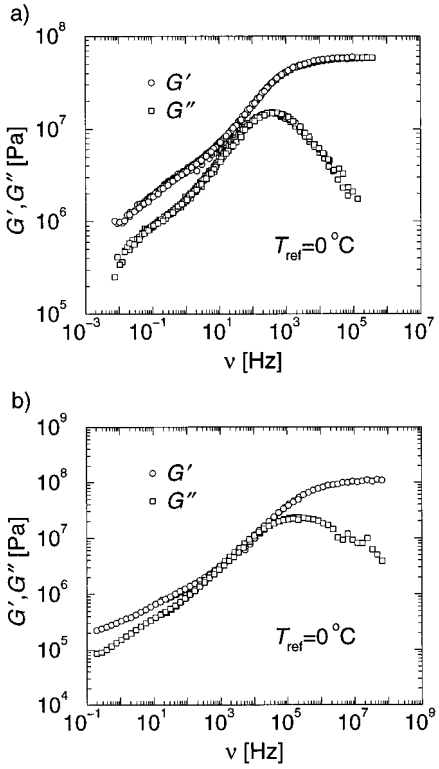

Figure 7. Master curves for the smectic A phase. (a) Sample A (the curves are obtained from the superposition of measurements taken at 16, 15, 13, 11, 10, 8, 6, 4, 0, −2, −6, −8, −9, −11, and −13 °C). (b) Sample B (the curves are obtained from the superposition of measurements taken at 0, −5, −10, −15, −20, and −26 °C).

The fit parameters found for sample A read $C_1^A \approx 2.0$ and $C_2^A \approx 10^2$ K and for sample B, $C_1^B \approx 10$ and $C_2^B \approx 370$ K. From that, we calculate the Vogel−Fulcher temperatures (i.e., the hypothetical temperatures where the viscosity is supposed to diverge) $T_V^A \approx -1.9$ °C and $T_V^B \approx -270$ °C and the activation temperatures, $T_A^A \approx 200$ °C and $T_A^B \approx 7800$ °C. The values obtained here for both samples differ very strongly. Although the values obtained for sample A suggest a Vogel−Fulcher temperature and therefore a glass transition above T_G and thus well inside the smectic A phase, the Vogel−Fulcher temperature observed for sample B is far below T_G. These at first surprising results obtained for T_V are most likely due to the isotropic−smectic A transition, which appears between the reference temperature and T_G. Therefore, the numerical data for T_V and T_A obtained for the isotropic phase have most likely no physical meaning.

The master curves describing the smectic A phase of both samples are plotted in Figure 7. Starting the discussion with the curves obtained for compound A leads one to observe three characteristic regimes: In the low-frequency regime (10^{-2} Hz $\lesssim \nu \lesssim 1$ Hz), a power law type behavior $G'(\nu) \propto \nu^{\zeta}$ appears to develop. The corresponding exponent assumes $\zeta^{\text{A}} = 0.28 \pm 0.02$. In this frequency regime, the loss modulus also seems to follow a power law $G''(\nu) \propto \nu^{\tilde{\zeta}}$, but with a slightly larger exponent $\tilde{\zeta}^{\text{A}} \approx 0.32 \pm 0.02$. Qualitatively, the same behavior is observed for sample B. Here, the exponents assume $\zeta^{\text{B}} = 0.29 \pm 0.02$ and $\tilde{\zeta}^{\text{B}} = 0.38 \pm 0.02$.

After a crossover region, we observe another regime, which can be described by an exponent α with $\alpha \approx 0.45 \pm 0.05$ in both samples. This region, however, is most

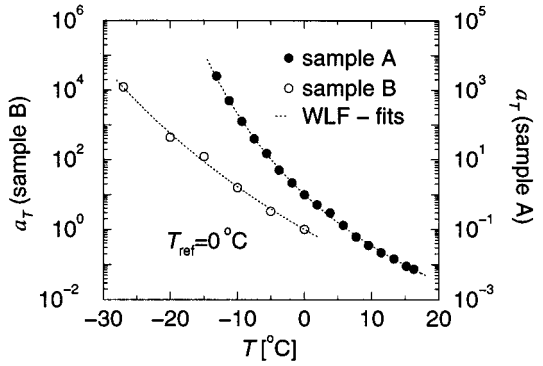

Figure 8. Shift factors a_T used for superposition of the curves in the smectic A phase and corresponding fit with the WLF law.

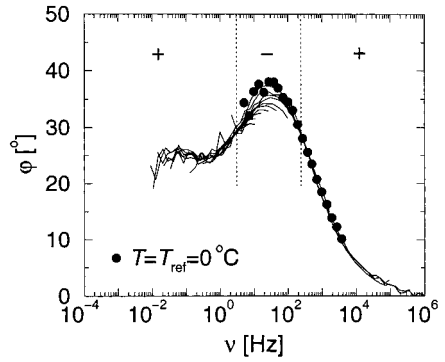

Figure 9. Master curves for the phase shift φ for sample A taken at the same temperatures as the master curves in Figure 7. The data for the reference temperature $T = T_{ref} = 0$ °C are represented by ● and all of the superimposed curves by solid lines. Because the experimental setup is more sensitive to low-frequency perturbations, the scatter in the low-frequency range is larger than that in the high-frequency range.

probably related to the α-processes slightly below the dynamic glass transition,[38] and is thus most likely not related to the liquid crystalline properties of the compounds, but is rather a result that should be found in all SCLCEs. Thus, we identify two characteristic regions in the master curves with a power-law-like shape, where the corresponding low-frequency exponents of the $G'(\nu)$ curves reach $\zeta \approx 0.30 \pm 0.05$ and with the high-frequency exponents $\alpha \approx 0.45 \pm 0.05$. These values are reproducible in all of the smectic compounds we have investigated up to now (see also Gallani et al.[26]). For very high frequencies, one finally arrives at the glassy plateau where $G'(\nu)$ approaches a constant value and $G''(\nu)$ has to go to zero.[34,35] It is important to mention here that the characteristic shape of the master curves we obtain for SCLCEs in their smectic phase as described above resembles those which Colby et al.[7] find for a SCLCP in its smectic phase (compare especially Figure 7 with Figure 3 in Colby et al.[7]). Even the numerical value for the "exponent" of $G'(\nu)$, which can be extracted from there is found to be $\zeta \approx 0.3$. In contrast to what Colby et al.[7] found for SCLCPs, samples A and B obey the WLF equation to a very high precision (Figure 8). The corresponding fit parameters obtained in the smectic A phase for sample A are $C_1^A \approx 7.9$ and $C_2^A \approx 44$ K and for sample B, $C_1^B \approx 11$ and $C_2 \approx 100$ K. From that, we calculate the characteristic temperatures $T_V^A \approx -44$, $T_A^A \approx 530$, $T_V^B \approx -100$, and $T_A^B \approx 2300$ °C. In contrast to what we have reported above for the isotropic phase, the values of T_V and T_A we obtain for the smectic phase resemble much more the ones usually reported for polymers;[35] that is, T_V is about 30−70 K below T_G and the activation temperature is in the range 700−2600 °C. But nevertheless, time−temperature superposition does not work perfectly in the smectic A phase, even though the master curves, especially those for sample A, as well as the WLF curve look very smooth. There are regions in the phase shift $\varphi(\nu)$ (Figure 9) where the superposition principle works fine (marked with "+"). The problematic region is 1 Hz $\lesssim \nu \lesssim$ 100 Hz where the cross-over between the two scaling regions occurs. Although this mismatch can hardly be seen in Figure 7, it becomes more transparent in the phase-shift plot. Here, the cross-over regime corresponds to the pronounced maximum marked with "−", which changes height as a function of temperature. Thus for superposition, this maximum has to be ignored.

Compression Measurements. As explained in Introduction and Motivation, the piezo-rheometers introduced above can also be used to measure the dynamic compression modulus E^*. In Figure 10, we present measurements of $E'(T)$ obtained for sample A for the interval 20 °C $\lesssim T \lesssim$ 120 °C, thus focusing on the important part in vicinity of the phase transition and on the isotropic phase. The measurements are taken at the excitation frequencies 1.4, 10, and 100 Hz and 1 kHz. The curves display the same characteristic behavior as $G'(T)$, that is, a steep decrease of $E'(T)$ in vicinity of T_{I-A} and a convergence to a frequency-independent value of $E'(T)$ far above the transition temperatures. The master curve for sample A in the isotropic phase is plotted in Figure 11. It shows that the time−temperature superposition principle works reasonably well for compression and high temperatures ($T \geq 85$ °C). For

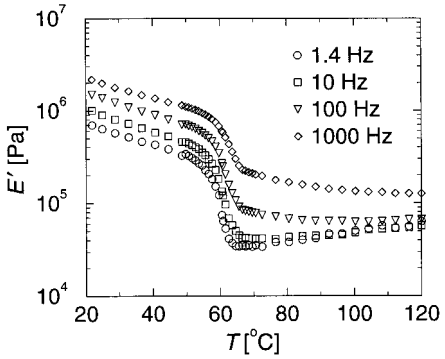

Figure 10. Temperature dependence of the storage modulus $E'(T)$ taken at $\nu = 1.4$, 10, and 100 Hz and 1 kHz for sample A.

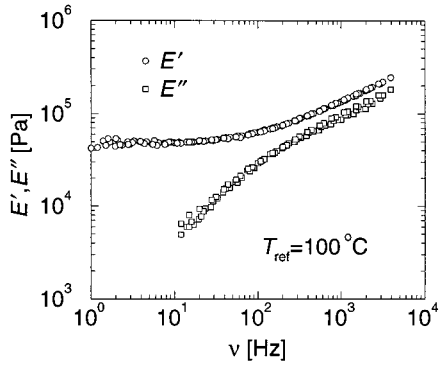

Figure 11. Master curves of E' and E'' in the isotropic phase for Sample A (the curves are obtained from the superposition of measurements taken at 100, 96, 92, 88, and 85 °C).

lower temperatures, however, there are significant deviations. Therefore, the frequency range attainable by superposition is smaller than the one investigated for shear in Figure 3. Nevertheless, $E'(\nu)$ shows the same qualitative behavior as the shear modulus, that is, a low-frequency plateau reflecting the permanent network and a scaling regime with an exponent close to 0.5.

Discussion of the Results. *Isotropic Phase.* To summarize the essential results obtained in the isotropic phase, we note three important features. First, the storage moduli $G'(\nu)$ as well as $E'(\nu)$ can be written in the following form:

$$G'(\nu) = G'_{st} + G'_{v}(\nu) \text{ and } E'(\nu) = E'_{st} + E'_{v}(\nu)$$

with the two frequency-independent contributions $G'_{st} \approx 10^4$ Pa and $E'_{st} \approx 4 \times 10^4$ Pa. These static contributions to the storage moduli are the consequence of the chemical crosslinks forming a three-dimensional permanent network, which suppresses the macroscopic flow in an elastomer. The ratio E'_{st}/G'_{st} determined in the hydrodynamic regime ($\nu \lesssim 10$ Hz) is on the order of 3−4. This value accounts quite well for what is expected for a Hookean elastic solid. The deviation from the expected value $2 \leq E'_{st}/G'_{st} < 3$ can be explained by the error (≈20%) associated with the determination of the piezoelectric constants of the transducers and the sample area and for E^* by the small precompression induced in the sample when it is installed in the setup.

Second, the dynamic contributions to the storage moduli are characterized by scaling laws $G'_v(\nu) \propto E'_v(\nu) \propto \nu^{0.5}$. The third observation, which is strongly related to this scaling behavior is the frequency-dependent behavior of the phase shift $\varphi(\nu)$. Above a characteristic frequency $\nu \gtrsim 10$ Hz, the phase shift $\varphi(\nu)$ increases; i.e., the response of the system is no longer hydrodynamic ($\omega\tau \ll 1$), and thus the relaxation time of the longest lived mode in the isotropic phase is on the order of 10^{-2}−10^{-1} s. For higher frequencies, an increasing number of modes appears frozen. For $\nu \gtrsim 10^3$ Hz, the phase shift φ assumes a constant value of 45° for shear. In this frequency regime, scaling with the exponent 0.5 is fully developed. Both an exponent of 0.5 and a phase shift $\varphi = 45°$ characterize a viscoelastic liquid, which can be described in the simplest case by the Rouse model.[39] The most general formulation of the Rouse model describes the motion of Brownian particles diffusing around randomly and interacting only locally with their nearest neighbors.[39] Following this picture, we may understand the nature of the viscoelastic response the SCLCEs show: they form bulky clusters of side groups (Rouse sequences) that are only weakly coupled to the polymeric backbone through their flexible, aliphatic spacers. These associations of side groups carry out micro−Brownian motion (a macroscopic flow is of course impossible, because of the permanent network) and interact mostly sterically. The backbone itself acts merely as a constant background giving rise to G'_{st} and E'_{st}.

However, the exponent 0.5, which we have found rather frequently (cf. also Gallani et al.[26]) in the isotropic phase of SCLCEs, is not universal, as has been shown by measurements performed on nonliquid crystalline elastomers with rigid and bulky side groups connected to the backbone via a flexible spacer.[40] Therefore, we present another possibility to explain the scaling behavior, which is closely related to the results recently obtained for SCLCPs.[4,41] There, the presence of transient clusters (spatial inhomogeneities) of macroscopic size (∼10−50 μm) results in a scaling law with an exponent of 0.6−0.7. These clusters (if they do also exist in SCLCEs) could represent the origin of the scaling law with the measured exponent of 0.5. The numerical difference in the value of the exponent of SCLCPs and SCLCEs (≈0.7 → 0.5) could be due to the influence of the permanent network on the spectrum of relaxation times of the transient clusters.

Both pictures imply a similar behavior for SCLCEs in their isotropic and their nematic phase, because both phases are essentially three−dimensionally fluid. The latter result is shown by Gallani et al.,[26] who demonstrate that time−temperature superposition works well across an isotropic−nematic transition. There, the compounds under investigation also exhibit an exponent of approximately 0.5 for both phases.

The Smectic A Phase and the Phase Transition to the Isotropic Phase. When comparing the master curves characterizing the isotropic phase (Figure 4) and the smectic A phase (Figure 7), respectively, the largest difference that is noticed is related to the low-frequency regime. Even at the lowest frequencies experimentally accessible, the measured value of $G'(\nu)$ is more than 1 order of magnitude higher than the value characterizing the permanent network plateau $G'_{st} = 10^4$ Pa in the isotropic phase. Assuming the validity of a power law with an exponent of 0.3 over the whole low-frequency regime and extrapolating the curves in Figure 7 to a value of $G'(\nu) \approx G'_{st}$ (obtained in the isotropic phase) gives a rough estimate for the lifetime of the longest lived modes of the system. For sample A, one arrives at a lifetime $\tau_A \approx 10^8$s (where T_{ref} is 20 K above T_G) or for sample B $\tau_B \approx 10^5$s (where T_{ref} is 30 K above T_G). These values are comparable to the ones reported in Colby et al.[7]

This drastic lifetime enhancement of the elastic modes in a smectic A polydomain SCLCE can be qualitatively understood by a simple picture: the mesogens linked to one specific polymeric backbone usually belong to different smectic layers or even different smectic domains. Consequently, different polymeric backbones are effectively connected via their sidegroups, which are trapped in different smectic layers or domains, respectively. The resulting network structure is in principle transient, but a complete relaxation of the applied stress could also be ruled out by steric hindrance and entanglements. Therefore, even a much longer lifetime of this transient smectic network as the extrapolated τ_A or τ_B, respectively, seems reasonable. Following the arguments given above, this additional contribution to the elastic moduli due to the transient smectic network is strongly influenced by the compression modulus of the smectic layers B (cf. Nishikawa et al.[21]) and thus is expected to be much larger than the shear modulus of the elastomer in its isotropic phase.

If the picture given above turns out to be applicable, the step of the $G'(T)$ curves (and $E'(T)$ curves, respectively) observed in vicinity of the phase transition is the natural consequence of the disappearance of the smectic layers at the phase transition. With these layers, the transient smectic network also disappears, and one merely probes the elastic modulus of the permanent network.

When comparing the heights of the steps found for samples A and B, one observes that the height obtained

for sample A is much bigger. This result fits well to the interpretation in terms of a transient smectic network, because only 25 mol % of the monomers of sample B carry mesogenic groups, whereas the mesogen fraction for sample A is 90 mol %. Therefore, the transient smectic network in sample A should be much stronger. This interpretation is also consistent with the numerical values obtained for the Vogel−Fulcher and the activation temperatures for both samples: because in both the transient smectic network and the glassy state the internal degrees of freedom appear frozen even at very low frequencies, these states are very similar. Therefore, the quantitative difference between the two states at T_G becomes smaller with increasing strength of the transient smectic network. Consequently, the numerical values obtained for T_V and T_A should be smaller for a stronger transient smectic network. This prediction is observed for our samples A and B.

Apart from the transient smectic network discussed above, the different polymeric backbones are of course chemically cross-linked. What will happen, if these permanent cross-links are absent? In this state, the material represents a SCLCP in its smectic A phase. However, there is no influence on the existence or the properties of the transient smectic network. If its contribution dominates over that of the permanent network, and that seems to be true in all cases, one will expect nearly the same dynamic behavior for SCLCEs and SCLCPs in their smectic phase. Therefore, this picture easily explains the similar shape of the master curves we obtained in the smectic A phase (Figure 7) and the one obtained by Colby et al. (cf. Figure 3 of Colby et al.[7]), even though both the polymeric backbone as well as the mesogens under investigation are totally different. Unfortunately, Colby et al.[7] do not show the temperature-dependent behavior of G' for this compound, but it is most likely that their compound also shows the step at the phase transition. Yamaguchi et al. also present rheological investigations on SCLCPs and thereby concentrate on a third family of compounds.[5,6] They present $G'(T)$ and $E'(T)$ measurements that also show the discussed step, which reflects the formation of the smectic layers, and as observed for sample B, the step is also hidden there by the dynamic glass transition for higher frequencies. Very recently Ortiz et al.[29] presented the first rheological experiments performed on smectic A liquid crystalline main-chain elastomers. In addition, in these systems, the step can be observed, which again fits well to our interpretation in terms of a transient smectic network.

We shall proceed with the discussion of the exponent characterizing the low-frequency regime of the master curve for the smectic A phase. The picture outlined above gives a qualitative understanding for the unusually large lifetime of the transient network in the smectic A phase. But nevertheless, the question of whether there exists a power law regime with an exponent $\zeta \approx 0.3$ for both $G'(\nu)$ and $G''(\nu)$ in the low-frequency regime cannot yet be answered conclusively. However, we should mention that we have observed the same slope for SCLCEs in their smectic phase (cf. also Gallani et al.). An exponent of 0.3 can also be read off the plots in Yamaguchi and Asada[6] and Colby et al.[7] for SCLCPs in their smectic A phase and thus seems to be a universal value of a smectic phase in both side-chain liquid crystalline polymers and elastomers.

When increasing the frequency further to $\nu \approx 10^2$ Hz, we arrive at a second scaling regime with an exponent $\alpha \approx 0.5$. As already mentioned above, we believe that this regime is due to the α relaxation process and is not related to the smectic phase. Therefore, we expect this behavior for frequencies slightly below those characterizing the dynamic glassy state to be universal for all of the side-chain liquid crystalline elastomers, no matter whether they are in their isotropic, nematic, or smectic phase.

4. Summary and Perspective

We have experimentally shown by dynamic shear and compression experiments carried out on different SCLCEs that the storage moduli $G'(\nu)$ and $E'(\nu)$ can be represented as the sum of two terms: one is independent of the frequency and reflects the presence of the three-dimensional permanent network, whereas the second depends on the frequency and gives rise to a scaling behavior ($G'_\nu(\nu) \propto E'_\nu(\nu) \propto \nu^\zeta$). In the isotropic phase, this exponent assumes the value $\zeta = 0.5$. Two possible mechanisms have been proposed to explain the origin of these scaling laws. The first rests on the numerical value of the exponent ($\zeta = 0.5$) and suggests that associations of mesogenic side groups carry out correlated diffusive motions and therefore represent a viscoelastic liquid of the Rouse type. The second assumes that the associations of mesogenic side groups give rise to transient elastic clusters of macroscopic size as they are always observed in SCLCPs.[4,41] In that case, $\zeta = 0.5$ should not be universal. Experiments that have been performed on an elastomer with nonliquid crystalline but sufficiently bulky side groups suggest this to be the case,[40] but other experiments are necessary to give a definite answer to this question.

Note that both interpretations are able to explain why the rheological behavior of SCLCEs does not change when an isotropic−nematic transition is crossed, an experimental fact that has recently been described in Gallani et al.[26]

The picture changes drastically when the system changes to a smectic phase, where we commonly find $\zeta \approx 0.3$ for the value of the exponent. There, the (one-dimensional) solid character of the smectic phase together with the geometrical restrictions the polymeric backbone imposes on the system are the most important reasons for the strong and most likely transient smectic network observed in the experiment. Usually the transient smectic network dominates over the permanent network and consequently leads to the very similar properties both a smectic SCLCE and a smectic SCLCP show in shear experiments. This could be verified by performing rheological experiments on the smectic A phases of a polydomain SCLCE and its underlying SCLCP in their smectic A phase. Both should show the same rheological behavior because of the dominant contribution of the transient smectic network.

Finally, we want to mention that the interpretation of the processes taking place in the smectic A phase is also valid for other two-dimensionally fluid smectic phases such as smectic C phases, because the model is only based on the existence of highly incompressible smectic layers but not on the relative orientation between the mesogens and the smectic layer normal.

Acknowledgment. We thank E. Rössler and P. E. Cladis for fruitful and stimulating discussions. We thank the Deutscher Akademischer Austauschdienst (312/pro-gg) and the Ministère des Affaires Etrangères (96096) through PROCOPE for support of this project. Partial support by the Deutsche Forschungsgemeinschaft is gratefully acknowledged.

References and Notes

(1) Finkelmann, H.; Ringsdorf, H.; Wendorff, J. H. *Makromol. Chem.* **1978**, *179*, 273.
(2) Reys, V.; Dormoy, Y.; Gallani, J. L.; Martinoty, P.; Le Barny, P.; Dubois, J. C. *Phys. Rev. Lett.* **1988**, *61*, 2340.
(3) Reys, V.; Dormoy, Y.; Collin, D.; Keller, P.; Martinoty, P. *J. Phys. II (Paris)* **1992**, *2*, 209.
(4) Gallani, J. L.; Hilliou, L.; Martinoty, P.; Keller, P. *Phys. Rev. Lett.* **1994**, *72*, 2109.
(5) Yamaguchi, T.; Asada, T. *Mol. Cryst. Liq. Cryst.* **1991**, *198*, 299.
(6) Yamaguchi, T.; Asada, T. *Mol. Cryst. Liq. Cryst.* **1992**, *214*, 1.
(7) Colby, R. H.; Gillmor, J. R.; Galli, G.; Laus, M.; Ober, C. K.; Hall, E. *Liq. Cryst.* **1993**, *13*, 233.
(8) de Gennes, P. G. *Compt. Rend. Acad. Sci. B* **1975**, *281*, 101.
(9) Pleiner, H.; Brand, H. R. *Mol. Cryst. Liq. Cryst.* **1991**, *199*, 407.
(10) Pleiner, H.; Brand, H. R. *Macromolecules* **1992**, *25*, 895.
(11) Brand, H. R.; Kawasaki, K. *J. Phys. II (Paris)* **1992**, *2*, 1789.
(12) Brand, H. R.; Kawasaki, K. *J. Phys. II (Paris)* **1994**, *4*, 543.
(13) Brand, H. R.; Kawasaki, K. *Physica A* **1994**, *208*, 407.
(14) de Gennes, P. G. *The Physics of Liquid Crystals*; Clarendon Press: Oxford, 1982.
(15) Finkelmann, H.; Kock, H.-J.; Rehage, G. *Makromol. Chem., Rapid Commun.* **1981**, *2*, 317.
(16) Küpfer, J.; Nishikawa, E.; Finkelmann, H. *Polym. Adv. Techn.* **1994**, *5*, 110.
(17) Finkelmann, H.; Brand, H. R. *Trends Polym. Sci.* **1994**, *2*, 222.
(18) Brand, H. R. *Makromol. Chem., Rapid Commun.* **1989**, *10*, 57.
(19) Olbrich, M.; Brand, H. R.; Finkelmann, H.; Kawasaki, K. *Europhys. Lett.* **1995**, *31*, 281.
(20) Küpfer, J.; Finkelmann, H. *Macromol. Rapid Commun.* **1991**, *12*, 717.
(21) Nishikawa, E.; Finkelmann, H.; Brand, H. R. *Macromol. Rapid Commun.* **1997**, *18*, 65.
(22) Nishikawa, E.; Finkelmann, H. *Macromol. Chem. Phys.* **1997**, *198*, 2531.
(23) Bergmann, G. H. F.; Finkelmann, H.; Percec, V.; Zhao, M. *Macromol. Rapid Commun.* **1997**, *18*, 353.
(24) Brand, H. R.; Kawasaki, K. *Macromol. Rapid Commun.* **1994**, *15*, 251.
(25) Oppermann, W.; Braatz, K.; Finkelmann, H.; Gleim, W.; Kock, H.-J.; Rehage, G. *Rheol. Acta* **1982**, *21*, 423.
(26) Gallani, J. L.; Hilliou, L.; Martinoty, P.; Doublet, F.; Mauzac, M. *J. Phys. II (Paris)* **1996**, *6*, 443.
(27) Hilliou, L. Thèse, Strasbourg, 1996, unpublished.
(28) Weilepp, J.; Stein, P.; Assfalg, N.; Finkelmann, H.; Martinoty, P.; Brand, H. R., to be published.
(29) Ortiz, C.; Wagner, M.; Bhargava, N.; Ober, C. K.; Kramer, E. J. *Macromolecules* **1998**, *31*, 8531.
(30) Forster, D. *Hydrodynamic Fluctuations, Broken Symmetry and Correlation Functions*; Benjamin: Reading, MA, 1975.
(31) Landau, L. D.; Lifshitz, E. M. *Elasticity Theory*; Pergamon Press: New York, 1959.
(32) As will be discussed by in an upcoming article, the monodomain analogue of the sample investigated here might exhibit an isotropic−nematic transition at $T_{I-N} = 65$ °C followed by a very narrow nematic phase and a nematic-to-smectic A transition in the region 58 °C $\lesssim T_{N-A} \lesssim$ 62 °C. These transition temperatures cannot be resolved by DSC measurements but follow indirectly from the thermoelastic behavior of the monodomain sample. Assfalg, N.; Finkelmann, H., to be published.
(33) Finkelmann, H.; Rehage, G. *Makromol. Chem., Rapid Commun.* **1980**, *1*, 31.
(34) Ferry, J. *Viscoelastic Properties of Polymers*; Wiley: New York, 1980.
(35) Strobl, G. *The Physics of Polymers*; Springer: Berlin, 1996.
(36) Degert, C.; Richard, H.; Mauzac, M. *Mol. Cryst. Liq. Cryst.* **1992**, *214*, 179.
(37) Leroux, N.; Mauzac, M.; Noirez, L.; Hardouin, F. *Liq. Cryst.* **1994**, *16*, 421.
(38) Rössler, E., private communications.
(39) Doi, M.; Edwards, S. F. *The Theory of Polymer Dynamics*; Clarendon Press: Oxford, 1986.
(40) Stein, P.; et al., to be published.
(41) Martinoty, P.; Hilliou, L.; Mauzac, M.; Benguigui, L. G.; Collin, D. *Macromolecules*, **1999**, *32*, 1746.

MA9900838